Proc. NIPR Symp. Antarct. Meteorites, 4, 144–162, 1991

PETROLOGY OF YAMATO-75261 METEORITE: AN ENSTATITE (EH) CHONDRITE BRECCIA

Hiroko NAGAHARA

Geological Institute, Faculty of Science, University of Tokyo, 3–1, Hongo 7-chome, Bunkyo-ku, Tokyo 113

Abstract: Yamato-75261 is a breccia with a non-porphyritic clast embedded in the partly porphyritic matrix. The clast consists mainly of closely packed fine-grained enstatite with interstitial material rich in Al. Metallic iron and troilite are rare. An anomalous Fe-Mn-Mg-Ca-Cr monosulfied, of which composition lies intermediate between alabandite in EL chondrites and niningerite in EH chondrites, occurs in the interstices of the clast. The heterogeneous matrix consists of enstatite, forsterite, glass, fine-grained materials, and rare troilite. Chemical compositions of bulk meteorite, clast, and matrix obtained by the broad beam analysis of a microprobe are highly fractionated. Both the clast and matrix are especially depleted in siderophile elements, which is in accordance with apparent depletion of metallic iron over the thin section. Aluminum, Fe, Na, Si, Ca, and S are enriched in the matrix portion; on the contrary, Mg is enriched in the clast. Texture, mineral assemblage, and mineral compositions along with oxygen isotopic compositions (T. K. MAYEDA and R. N. CLAYTON; Papers presented to the 14th Symposium on Antarctic Meteorites, Tokyo, Natl Inst. Polar Res., 172, 1989) suggest that Y-75261 is a breccia related to enstatite chondrites. The CaO content of enstatite, Ni, Si, and P contents of kamacite, and Ti and Cr contents of troilite indicate a closer affinity to EH chondrites than to EL's in spite of the intermediate composition of the sulfide.

1. Introduction

Yamato-75261 has been tentatively classified as a "unique meteorite" (YANAI and KOJIMA, 1985), probably because of highly magnesian nature of olivine and pyroxene ($Fa_{0-0.9}$ and $Fs_{0.1-0.5}$). The meteorite was studied as part of consortium on "unique meteorites". Most of the meteorites studied in the consortium are characterized by Mg/(Mg+Fe) ratios for olivine and pyroxenes intermediate between E and H chondrites, non-chondritic texture and essentially chondritic compositions like Lodran, Acapulco, and Pontlyfni (NAGAHARA *et al.*, 1990). Present petrological study has revealed that Y-75261 is not related to those meteorites, but is related to enstatite chondrites.

Oxygen isotopic compositions of Y-75261 have been reported, $\delta^{18}O=+5.76\%$ and $\delta^{17}O=+2.73\%$ (MAYEDA and CLAYTON, 1989). MAYEDA and CLAYTON (1989) suggested that Y-75261 may be an winonaite.

Y-75621 is a small meteorite, originally only 0.59 g in weight, which is too small to allocate the combined studies including chemical analysis. In the present study, a polished thin section of Y-75261, 51–2 (2×1.5 mm) was petrologically studied.

2. Analytical Methods

An electron microprobe with wave length dispersive crystals, JEOL JCXA 733 Mk-II and a scanning electron microscope, JEOL JSM840 equipped with an energy dispersive spectrometer LINK-SYSTEM AN10000, in the Geological Institute of the University of Tokyo were used for mineral analyses and bulk chemical analysis. Accelerating voltage of 15 kV, sample current of 12 and 1 nA, and counting time of 30 and 100 s were used or EPMA and EDS analyses, respectively. Standard ZAF corrections were applied for silicates and opaque minerals.

For the bulk composition of the sample, the broad beam (about 50×40 μm) analytical technique with the SEM-EDS was applied, whereby the sample was moved to cover the desired portion for 300 s. Since it is impossible to avoid cracks and areas outside of the thin section, the total of the analysis was within 93 and 98%. They were normalized to 100%. Elemental distribution of the sample was obtained with the mapping program of the microprobe operated at the sample current of 120 nA counting time of 60 μm s, and pixcel size of 5 μm$\times$5 μm.

3. Texture

Y-75261 is very fine-grained, hence it appeares almost opaque and each mineral is indistinguishable under an optical microscope. Figure 1a is an SEM-BEI photograph of Y-75261: the internal dark portion is a clast and the lighter portion surrounding the clast is the matrix. Enlarged views of the clast are shown in Figs. 1b and 1c, and those of the matrix are in Fig. 2.

The clast consists mostly of closely packed rectangular enstatite grains, about 10 to 20 μm in size, which have cleavages or partings parallel possibly to (001) (Fig. 1c), with a lesser amount of interstitial material. Opaque minerals such as metallic iron and troilite are very rare. Interstices of enstatite grains are occupied with glass or amorphous material(s) rich in Al which looks dark in the BEI photographs (Fig. 1c). The interstitial material is highly heterogeneous, the Al_2O_3 content ranging from 40 to 80 wt%, and smaller amonunts of SiO_2 (7–17 wt%), FeO (1–9), MgO (4–12), and CaO (0.4–12) are also variable (Table 1). Highly heterogeneous composition suggests that the material may be a fine-grained mixture of two or more phases. The S content is also variable, which may be due to presence of small sulfide grain(s). The clast is partly clastic as well as the matrix, where enstatite and interstitial material are finer-grained in a vein-like feature, showing a possibility that they were shocked *in situ*.

The matrix is highly heterogeneous. It is partly porphyritic with phenocrysts of forsterite and enstatite embedded in the clear glassy groundmass (Fig. 2a) and the phenocrysts often form aggergates (Fig. 2b). The glassy matrix is partly clastic (Fig. 2c). Groundmass of the porphyritic matrix can be divided into two types: one is clear glass accompained with porphyritic phenocrysts and the other is very fine-grained material, probably aggregates of several mineral phases (Fig. 2d).

The clear glassy groundmass is always in the porphyritic portion of the matrix with phenocrysts of enstatite and forsterite. It consists mainly of SiO_2 (57–63 wt%)

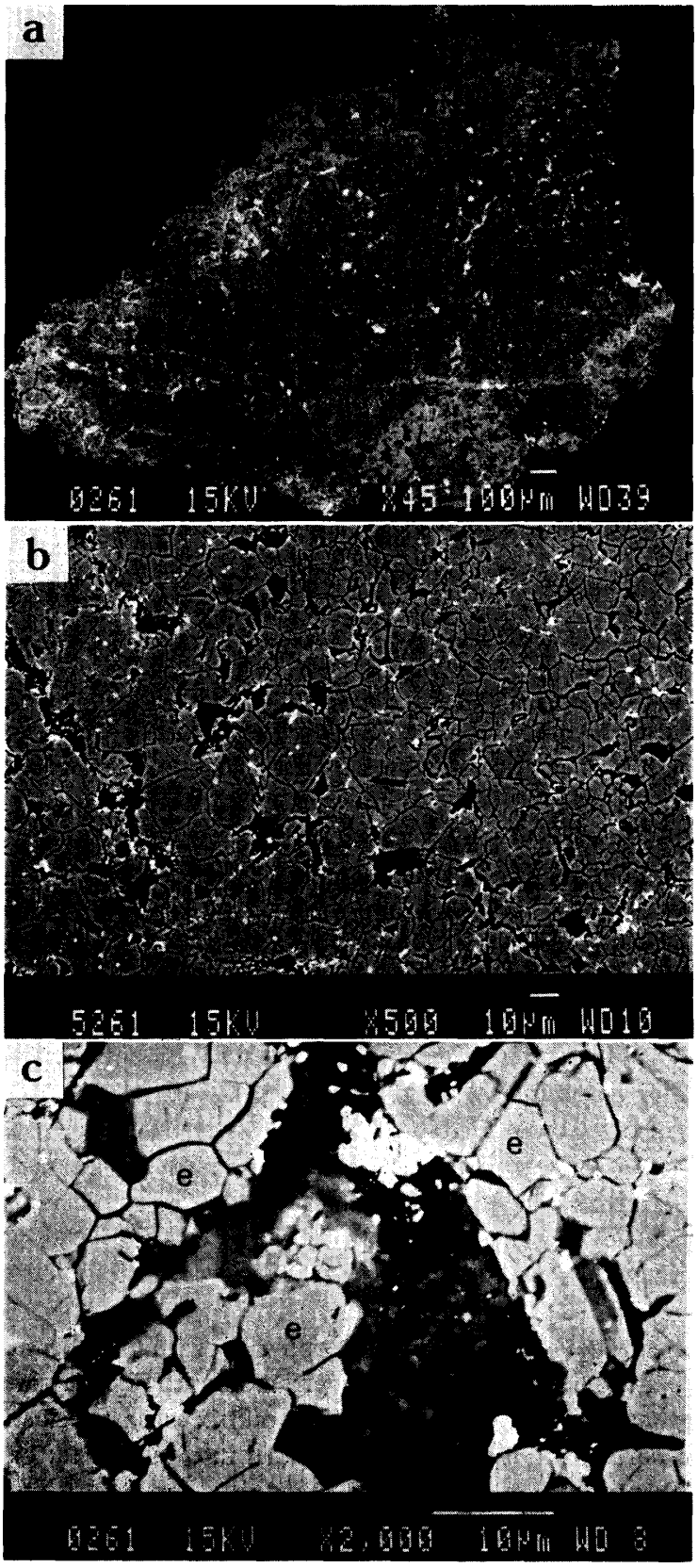

Fig. 1. SEM backscattered electron images (BEI) of Y-75261 meteorite.

a. Overview of the thin section studied. The inner dark portion is a clast and the outer light portion is matrix.

b. Texture of the clast. Closely packed rectangular enstatite (gray) and interstitial material (black).

c. Enlarged view of (b). Crystals are exculusively enstatite (e) with cleavages parallel probably to (001) and the interstitial material appears to be amorphous (am).

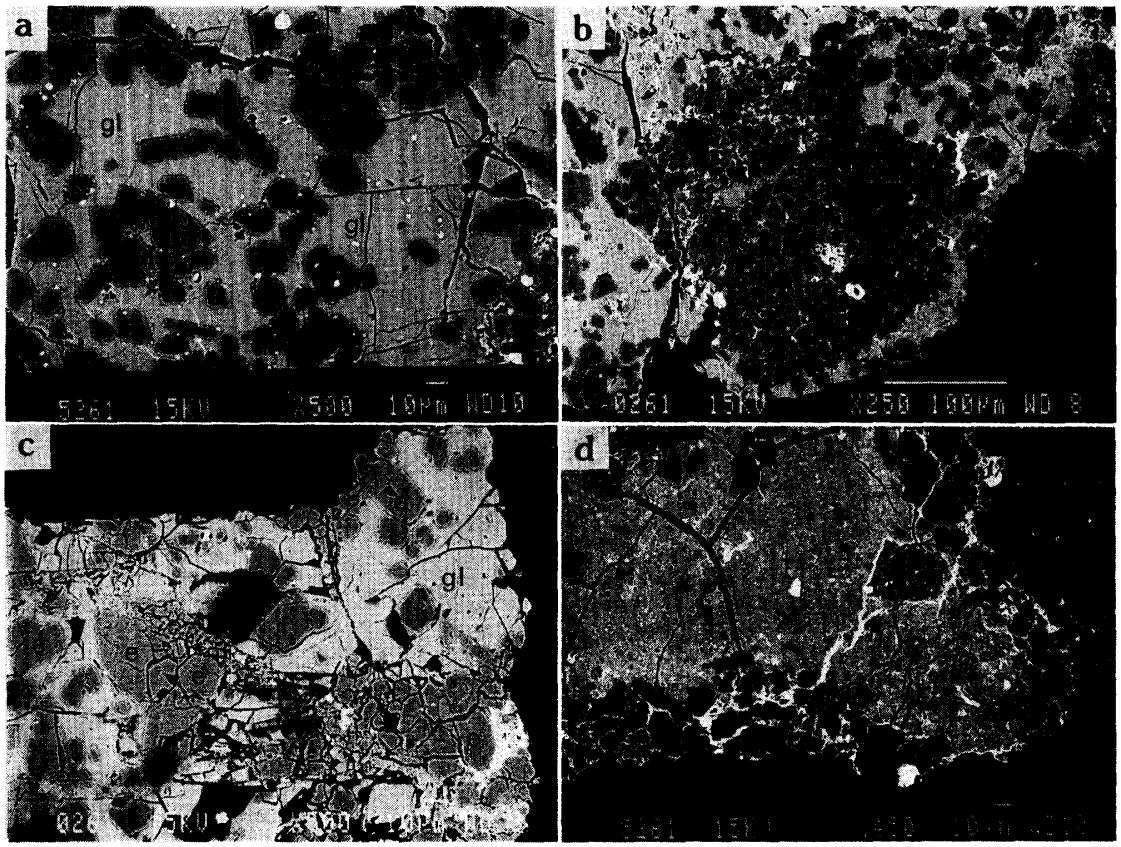

Fig. 2. BEI photographs showing texture of the matrix of Y-75261.

a. Porphyritic matrix with phenocrysts of forsterite (f) and enstatite (e) embedded in the clear glassy groundmass (gl). Bright spots are mostly troilite.

b. An aggregate of phenocrysts in the porphyritic matrix, which is mostly forsterite.

c. Partly clastic matrix suggestive of in situ crushing by a shock. The clastic crystals are mostly enstatite with lesser amount of forsterite.

d. Fine-grained portion of the matrix. It is highly heterogeneous and not known whether it is amorphous or crystalline. Bright veins contain Fe, Ni, and S.

Table 1. Representative chemical composition of the interstitial material of the clast in Y-75261. One set of data represents one analysis for different locations.

	SiO_2	Al_2O_3	FeO	MnO	MgO	CaO	Na_2O	Cr_2O_3	S	Total
1	7.11	76.91	1.41	0.00	4.55	1.59	0.16	0.00	0.53	92.53
2	17.56	42.65	1.39	0.46	11.44	12.01	0.00	0.00	0.55	86.34
3	10.15	55.33	8.94	0 00	6.53	0.41	0.00	0.00	1.59	83.75
4	9.99	51.93	18.31	0 00	6.64	1.19	0.00	0.38	6.48	98.16
5	17.20	60.30	1.14	0.00	11.71	1.29	0.00	0.00	0.29	92.07
6	10 07	72.18	0 00	0 00	7.17	0.54	0 00	0.00	0 24	90.32
7	14.77	61.55	0.00	0.00	12.03	0.53	0.48	0.00	0.33	89.86
8	10.88	59.39	0.40	0.00	9.41	0.59	0.45	0 00	0.35	81.64
9	11.53	57.31	1.99	0.00	7.49	0.19	0.00	0.00	1.21	80.32
10	2.04	71.32	0.45	0.00	3.82	0.67	0.36	0.00	0.36	78.66

Table 2. Representative chemical composition of the groundmass of the matrix in Y-75261.

	SiO_2	Al_2O_3	FeO	MgO	CaO	Na_2O	S	K_2O	Cr_2O_3	NiO	Total
1 clear 1	62 72	19.39	0 00	3.54	5.76	5.34	1.78	0.40	0.00	0.00	98.93
2 clear 1	60.81	19.25	0.41	4.06	6.70	4.69	2.60	0.33	0.00	0.00	98.86
3 clear 1	61.83	19.18	0.00	3.77	6.27	4.40	2.15	0.46	0.00	0.00	98.05
4 clear 2	57.56	20.39	0.50	4.71	7.34	4.84	3.27	0.39	0.00	0.00	99.00
5 clear 2	56.69	19.64	1.03	6.85	6.44	4.42	3.11	0.40	0.00	0.00	98.58
6 clear 2	58.43	20.26	0.00	4.49	6.93	4.99	3.03	0.38	0.00	0.00	98.51
7 clear 3	62.83	18.38	0 00	3.18	6.87	4.75	0.82	0.45	0.00	0.00	97.28
8 clear 3	60.88	19.47	0.65	3.69	6.65	4.75	1.89	0.42	0.00	0.00	98.39
9 clear 3	62.57	19.75	0.00	3.81	6.65	4.92	1.36	0.43	0.00	0.00	99.49
10 f. g. 1	39.96	5.85	17.67	15.96	0.68	0.59	1.29	0.54	0.46	0.98	83.98
11 f. g. 1	40.88	6.49	19.24	14.60	0.49	0.00	0.74	0.52	0.39	1.34	84.69
12 f. g. 2	38.40	5.59	22.42	16.01	0.56	0.86	1.04	0.40	0.53	1.13	86.94
13 f. g. 2	38.92	5.91	21.87	19.45	0.52	0.83	0.81	0.36	0.00	2.01	90.67
14 f. g. 3	39.00	3.37	15.34	21.42	0.00	0.58	1.63	0.24	0.00	0.79	82.37
15 f. g. 3	37.80	3.19	16.43	20.52	0.21	0.00	2.10	0.18	0.84	1.12	82.39

Clear: clear: clear glassy portion of the porphyritic groundmass, f. g.: finegrained portion of the matrix as shown in Fig. 2d. The same numbers in the left column represent the neighboring area.

and Al_2O_3 (18–21) with lesser amounts of MgO (3–7), CaO (6–7), Na_2O (4–5), and sulfur (1–3% as S), which is nearly homogeneous in a scale of a few hundreds μm but is heterogeneous in a scale of several hundreds μm (Table 2). The chemical state of sulfur is not known. It may be, however, plausible that sulfur is contained in tiny globules of sulfide(s) because there are various sulfides in other portions of the glass. Hence, here it is shown as pure sulfur, tentatively. It is notable that the glass does not have Fe though it has a considerable amount of sulfur, suggesting that the sulfur in the glass may have been derived from sulfide(s) other than troilite such as niningerite and/or oldhamite. Highly silica rich composition may be due to an origin as a residual liquid after crystallization of forsterite (and enstatite). Tiny heavy (bright on the backscattered images) blebs are dispersed in the glass portion, and most of them are troilite. The troilite may have crystallized from an immiscible liquid. Such a clear glass is rarely found in enstatite chondrites. Chondrules in EH3 chondrites, Y-691 and Qingzhen contain clear glass, but are different from the glass in Y-75261 in that they are rich in the albite component (NAGAHARA, unpubl. data).

The clear glassy groundmass is partly penetrated by Fe-rich veins. The veins are heterogeneous and consist mostly of Fe with small amounts of S and Ni and lesser amounts of Si and Mg. They form a network surrounding grains. The veins may originally have been metallic iron which had oxidized during melting with lesser amounts of troilite and enstatite.

The matrix is partly clastic, and the clastic minerals are exclusively enstatite (Fig. 2c). Grain size ranges from submicrons to several tens μm, and the clastic porition is distributed heterogeneously in the matrix. Occurrence of the clastic matrix is similar to that in the clast.

The groundmass of matrix is partly very fine-grained and heterogeneous; it may

consists of aggergates of several mineral phases (Fig. 2d) although each mineral is indistinguishable even at high magnification with SEM. The chemical composition of the fine-grained portion is different from that of the clear glassy groundmass in that the former contains a considerable amount of Fe (Table 2). It is not rich in SiO_2 as the glassy groundmass is, SiO_2 ranging from 38 to 41 wt%. Aluminum (5–7), FeO (15–23), and MgO (14–20) are also variable (Table 2). The heterogeneity is mainly in the Al/(Si+Fe+Mg) ratio and the amount of alkalies (Na_2O and K_2O) and sulfur, which may be well understood if the heterogeneity is derived from a different mixing ratio of enstatite and Al-rich interstitial material of the clast. This in turn suggests that the matrix was formed from the clast-like material.

4. Mineralogy

4.1. Olivine

Olivine is rarely found in the clast, and it is in the porphyritic portion of the matrix which usually accompanies clear glassy groundmass. It is rectangular euhedral, being 10 to 20 μm in size (Fig. 2a). They are highly magnesian forsterite, Fo ranging from 99.8 to 99.9, with trace CaO (0.1 wt%). The concentrations of other elements such as MnO, Al_2O_3, Cr_2O_3, and NiO are below 0.1 wt%, mostly below 0.05 wt%. Although they look to be zoned in the very rim of each grain of BEI photographs (Figs. 2a and 2c), zoning is not detectalbe with a microprobe. Rare iron-bearing olivine (Fo_{91}) in the clast accompanies the monosulfide described below (Table 3). The occurrence and chemical composition of the glass indicate that the forsterite crystallized from a melt probably formed by a shock; that is, the forsterite is secondary.

Table 3. Representative chemical composition of olivine in Y-75261.

	SiO_2	Al_2O_3	FeO	MnO	wt% MgO	CaO	Cr_2O_3	NiO	Total	
1 matrix	42.83	0.07	0.09	0.04	57.01	0.04	0.03	0.04	100.15	
2 matrix	43.01	0.02	0.09	0.00	57.29	0.10	0.00	0.05	100.58	
3 matrix	43.14	0.02	0.11	0.07	57.02	0.07	0.00	0.05	100.52	
4 matrix	43.29	0.09	0.16	0.04	56.94	0.09	0.05	0.00	100.70	
5 matrix	43.23	0.07	0.14	0.01	57.13	0.09	0.00	0.00	100.68	
6 clast	40.80	0.00	8.58	0.00	48.78	0.37	0.76	0.00	99.45	
7 clast	39.83	0.00	11.87	0.00	45.63	0.32	0.50	0.00	98.23	
	Si	Al	Fe	Mn	cation Mg	Ca	Cr	Ni	Sum	XMg
1 matrix	1.002	0.002	0.002	0.001	1.988	0.001	0.001	0.001	2.998	0.999
2 matrix	1.002	0.001	0.002	0.000	1.990	0.000	0.000	0.001	2.998	0.999
3 matrix	1.005	0.001	0.002	0.002	1.981	0.002	0.000	0.001	2.994	0.999
4 matrix	1.007	0.002	0.003	0.001	1.974	0.002	0.001	0.000	2.992	0.999
5 matrix	1.006	0.002	0.003	0.000	1.981	0.002	0.000	0.000	2.993	0.999
6 clast	1.001	0.000	0.176	0.000	1.784	0.010	0.015	0.000	2.990	0.910
7 clast	1.004	0.000	0.250	0.000	1.714	0.010	0.010	0.000	2.991	0.872

1–5: porphyritic phenocrysis in the matrix, 6–7: iron-bearing olivine in the clast. One analysis represents one grain except for 6–7 which are for the same crystal.

4.2. *Pyroxene*

Pyroxene is the main constituent of Y-75261, occupying almost 70% of the thin section studied. It is euhedral to anhedral in the clast where grains with a similar size are closely packed (Fig. 1b). Pyroxene in the matrix exhibits three occurrences:

Table 4. Representative chemical composition of pyroxene in Y-75261.

	wt%											
	SiO_2	Al_2O_3	TiO_2	FeO	MnO	MgO	CaO	Na_2O	Cr_2O_3	V_2O_3	Total	XMg
1 matrix	59.89	0.49	0.03	0.05	0.03	39.50	0.26	0.02	0.02	0.03	100.32	0.9990
2 matrix	59.90	0.46	0.00	0.07	0.04	39.88	0.26	0.00	0.04	0.00	100.65	0.9985
3 matrix	59.87	0.32	0.01	0.06	0.07	39.68	0.19	0.01	0.03	0.03	100.27	0.9980
4 matrix	59.69	0.51	0.03	0.04	0.06	39.50	0.29	0.01	0.04	0.02	100.19	0.9985
5 matrix	59.93	0.15	0.00	0.35	0.00	39.96	0.20	0.02	0.02	0.06	100.69	0.9950
6 matrix	59.95	0.11	0.03	0.31	0.04	39.99	0.20	0.02	0.01	0.01	100.67	0.9950
7 matrix	60.10	0.31	0.01	0.35	0.02	39.74	0.19	0.01	0.00	0.02	100.75	0.9944
8 matrix	60.35	0.10	0.02	0.24	0.01	39.66	0.18	0.00	0.00	0.01	100.57	0.9965
9 matrix	60.50	0.51	0.00	0.28	0.03	39.56	0.26	0.02	0.01	0.00	101.17	0.9954
10 matrix	59.98	0.36	0.01	0.17	0.03	39.74	0.19	0.00	0.03	0.00	100.51	0.9970
11 clast	59.89	0.09	0.00	0.12	0.03	39.91	0.23	0.00	0.04	0.00	100.31	0.9980
12 clast	59.58	0.09	0.00	0.10	0.01	39.80	0.25	0.00	0.01	0.00	99.84	0.9985
13 clast	60.33	0.10	0.03	0.19	0.00	39.91	0.23	0.02	0.02	0.00	100.83	0.9975
14 clast	60.26	0.10	0.00	0.12	0.01	39.80	0.19	0.00	0.02	0.01	100.51	0.9985
15 clast	59.53	0.08	0.04	0.11	0.01	39.88	0.22	0.02	0.00	0.00	99.89	0.9985
16 clast	60.23	0.09	0.01	0.12	0.01	39.81	0.23	0.01	0.02	0.00	100.53	0.9985
17 clast	60.49	0.10	0.00	0.09	0.02	39.99	0.22	0.00	0.00	0.00	100.91	0.9980
18 clast	59.94	0.05	0.00	0.13	0.02	39.55	0.19	0.00	0.02	0.02	99.92	0.9975
19 clast	60.27	0.11	0.01	0.13	0.03	39.96	0.19	0.01	0.00	0.03	100.74	0.9975
20 clast	59.54	0.21	0.00	0.24	0.04	39.88	0.18	0.01	0.05	0.00	40.61	0.9960

	Cation at O=6											
	Si	Al	Ti	Fe	Mn	Mg	Ca	Na	Cr	V	Total	Mg+Fe
1 matrix	1.996	0.019	0.001	0.001	0.001	1.963	0.009	0.001	0.000	0.001	3.992	1.965
2 matrix	1.991	0.002	0.000	0.002	0.001	1.976	0.009	0.000	0.001	0.001	3.983	1.979
3 matrix	1.997	0.012	0.000	0.002	0.002	1.973	0.007	0.001	0.001	0.001	3.996	1.977
4 matrix	1.993	0.020	0.001	0.001	0.002	1.966	0.010	0.001	0.001	0.001	3.996	1.969
5 matrix	1.994	0.006	0.000	0.010	0.000	1.981	0.007	0.001	0.001	0.002	4.002	1.991
6 matrix	1.995	0.004	0.001	0.009	0.001	1.983	0.007	0.001	0.000	0.000	4.001	1.993
7 matrix	1.997	0.012	0.000	0.010	0.001	1.968	0.007	0.001	0.000	0.001	3.997	1.979
8 matrix	2.006	0.004	0.000	0.007	0.000	1.965	0.006	0.000	0.000	0.000	3.988	1.972
9 matrix	2.001	0.020	0.000	0.008	0.001	1.950	0.009	0.002	0.000	0.000	3.991	1.959
10 matrix	1.996	0.014	0.000	0.005	0.001	1.972	0.007	0.000	0.001	0.000	3.996	1.978
11 clast	1.998	0.004	0.000	0.003	0.001	1.984	0.008	0.000	0.001	0.000	3.999	1.988
12 clast	1.997	0.004	0.000	0.003	0.000	1.988	0.009	0.000	0.000	0.000	4.001	1.991
13 clast	2.002	0.004	0.001	0.005	0.000	1.974	0.008	0.001	0.000	0.000	3.995	1.979
14 clast	2.004	0.004	0.000	0.003	0.000	1.973	0.007	0.000	0.001	0.000	3.992	1.976
15 clast	1.995	0.003	0.001	0.003	0.000	1.992	0.008	0.001	0.000	0.000	4.003	1.995
16 clast	2.004	0.004	0.000	0.003	0.000	1.974	0.008	0.001	0.001	0.000	3.995	1.977
17 clast	2.004	0.004	0.000	0.003	0.001	1.975	0.008	0.000	0.000	0.000	3.995	1.979
18 clast	2.006	0.002	0.000	0.004	0.001	1.973	0.007	0.000	0.001	0.001	3.995	1.978
19 clast	2.001	0.004	0.000	0.004	0.001	1.978	0.007	0.000	0.000	0.001	3.996	1.983
20 clast	1.991	0.008	0.000	0.007	0.001	1.988	0.006	0.001	0.001	0.000	4.003	1.996

1–10: matrix, 11–20: clast. One analysis represents one grain.

one is porphyritic euhedral phenocryst with forsterite, which is embedded in the clear glass, the second is similar to pyroxene in the clast where euhedral to anhedral grains are closely packed, and the third is clastic. All of them are highly magenesian, as well as olivine, and contain very low concentrations of other elements including FeO, CaO, and MnO. Since their optical properties are difficult to determine under an optical microscope because of small grain sizes, the crystal structure of the pyroxene is not known. The facts that they are very low in CaO and that the cleavages or partings typically developed in the pyroxenes are parallel to (001), however, suggest that the pyroxene could be monoclinic, that is, clinoenstatite. If it is the case, the pyroxene should have crystallized above 1000°C and cooled rapidly.

The pyroxenes in the clast and matrix are chemically similar but are distinguishable

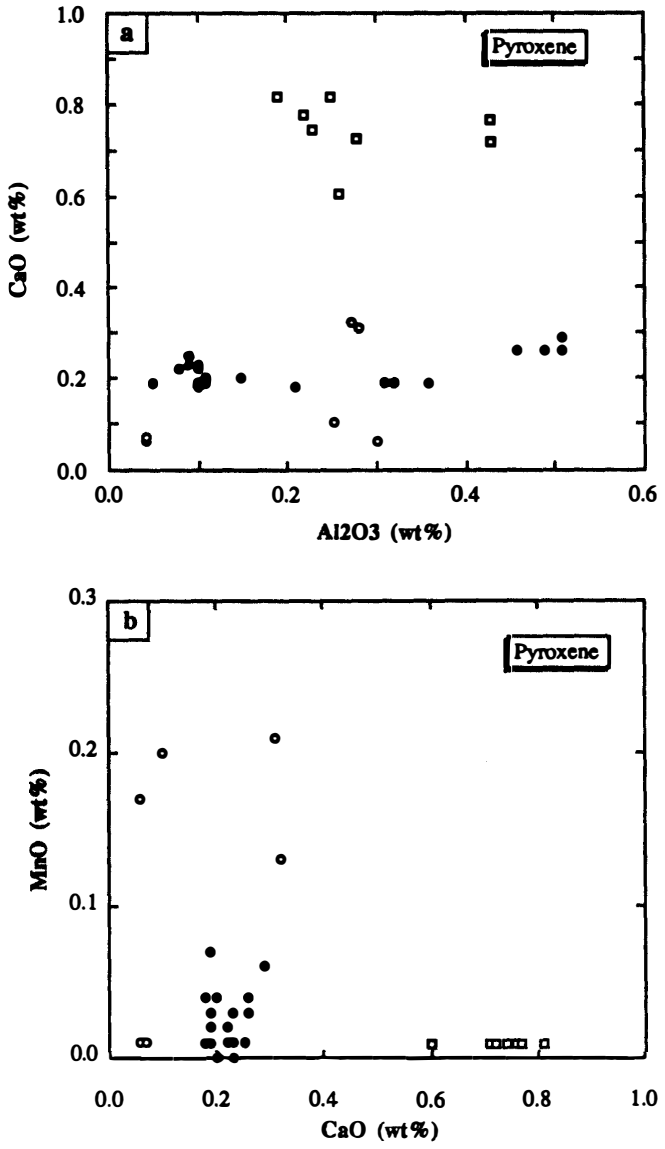

Fig. 3. The relationships between Al_2O_3 and CaO and between CaO and MnO contents of enstatite in Y-75261 in comparison with enstatites in EH and EL chondrites (data from KEIL, 1968). Closed circle: Y-75261, open circle: EH chondrites, open square: EL chondrites.

with respect to the Al_2O_3 content. The Al_2O_3 content of enstatite in the clast is mostly less than 0.1 wt% and that in the matrix is higher (between 0.1 and 0.5 wt%) (Table 4). Concentrations of other elements of pyroxenes in the clast and matrix, such as SiO_2, TiO_2, FeO, MnO, MgO, CaO, Na_2O, and Cr_2O_3, are almost the same.

Although the Al_2O_3 contents in pyroxenes in the clast and matrix show slight variations, the relationships among CaO, Al_2O_3 and MnO show that the pyroxenes in Y-75261 are chemically similar to EH chondrites but not to EL chondrites (Fig. 3). Iron content cannot be used as an indicator for genetic relationships because it varies easily with the redox state. Figure 3 exhibits that the composition of pyroxenes in Y-75261 is within the variational range of those in EH chondrites.

4.3. Metal and sulfides

As mentioned before, opaque minerals are scarce in Y-75261; they are kamacite and two sulfides, troilite and an unknown monosulfide (Fe, Mn, Mg, Ca, Cr) S. No

Table 5. Representative chemical composition of opaque minerals in the clast in Y-75261.

	wt%										
	Fe	Ni	Co	Si	Ti	Cr	Mg	Mn	Ca	S	Total
1 Kam	90.40	4.70	0.71	3.78	0.00	0.00	0.00	0.00	0.00	0.00	99.59
2 Kam	90.50	4.86	0.87	3.73	0.00	0.00	0.00	0.00	0.00	0.00	99.96
3 Tro	60.70	0.00	0.00	0.00	0.00	2.17	0.00	0.00	0.00	36.30	99.17
4 Tro	60.60	0.00	0.00	0.00	0.27	2.12	0.00	0.00	0.00	36.70	99.69
5 Tro	61.40	0.00	0.00	0.00	0.39	1.93	0.00	0.00	0.00	36.30	100.02
6 Tro	58.40	0.00	0.00	0.00	0.30	2.46	0.00	0.00	0.00	36.90	98.06
7 Tro	58.43	0.00	0.00	0.00	0.26	2.31	0.00	0.00	0.00	36.50	97.50
8 Tro	57.57	0.00	0.00	0.00	0.50	3.34	0.00	0.00	0.00	37.50	98.91
9 M. S.	29.25	0.00	0.00	0.00	0.00	0.63	10.52	14.21	1.94	40.56	97.11
10 M. S.	28.67	0.00	0.00	0.00	0.00	0.99	7.56	21.20	2.04	40.31	100.77
11 M. S.	28.04	0.00	0.00	0.00	0.00	0.77	7.55	21.51	2.06	39.66	99.59
12 M. S.	32.40	0.00	0.00	0.00	0.00	1.05	9.88	12.23	3.01	41.27	99.84
13 M. S.	30.34	0.00	0.00	0.00	0.00	1.64	8.27	15.09	2.89	40.49	98.72
14 M. S.	29.46	0.00	0.00	0.00	0.00	1.65	8.47	15.64	2.97	40.68	98.87
	atom %										
	Fe	Ni	Co	Si	Ti	Cr	Mg	Mn	Ca	S	Total
1 Kam	87.61	4.33	0.66	7.28	0.00	0.00	0.00	0.00	0.00	0.00	99.88
2 Kam	87.46	4.46	0.80	7.17	0.00	0.00	0.00	0.00	0.00	0.00	99.89
3 Tro	47.98	0.00	0.00	0.00	0.00	1.85	0.00	0.00	0.00	50.01	99.84
4 Tro	47.46	0.00	0.00	0.00	0.24	1.78	0.00	0.00	0.00	50.08	99.56
5 Tro	47.99	0.00	0.00	0.00	0.36	1.62	0.00	0.00	0.00	49.45	99.42
6 Tro	46.20	0.00	0.00	0.00	0.28	2.09	0.00	0.00	0.00	50.87	99.44
7 Tro	46.40	0.00	0.00	0.00	0.24	1.97	0.00	0.00	0.00	50.50	99.11
8 Tro	44.85	0.00	0.00	0.00	0.45	2.79	0.00	0.00	0.00	50.87	98.96
9 M. S.	20.59	0.00	0.00	0.00	0.00	0.48	17.02	10.17	1.90	49.75	99.90
10 M. S.	20.20	0.00	0.00	0.00	0.00	0.75	12.25	15.19	2.01	49.49	99.88
11 M. S.	19.97	0.00	0.00	0.00	0.00	0.59	12.35	15.57	2.05	49.20	99.72
12 M. S.	22.29	0.00	0.00	0.00	0.00	0.77	15.62	8.55	2.89	49.47	99.61
13 M. S.	21.47	0.00	0.00	0.00	0.00	1.25	13.45	10.85	2.85	49.91	99.77
14 M. S.	20.70	0.00	0.00	0.00	0.00	1.24	13.67	11.17	2.91	49.78	99.46

1–2: kamacite, 3–8: troilite, 9–14: monosulfide. One analysis represents one grain.

taenite, schreibersite, oldhamite, niningerite, alabandite and daubreelite has been found.

A few kamacite grains are found in the clast, which are about 10×20 μm and surrounded by enstatite grains. They are poor in Fe (90.5 wt%) and Ni (4.8 wt%) and rich in Si (3.8 wt%) (Table 5). Such an Si-rich kamacite is typical in EH chondrites (average 3.3 wt%; KEIL, 1968) and it is higher than that in EL chondrites (average 1.3 wt%; KEIL, 1968) (Fig. 4a). Phosphorous content in kamacites in Y-75261 is about 0.1–0.2 wt%, which is within the compositional range of kamacite, but is also close to those in EL's (Fig. 4b). In summary, kamacite in Y-75261 has closer affinity to EH's than to EL's mostly because of the Ni-Si relationships.

Troilite is contained in both the clast and matrix either as an isolated grain or coexistence with the monosulfide. It has nearly the same size as metal grains, mostly

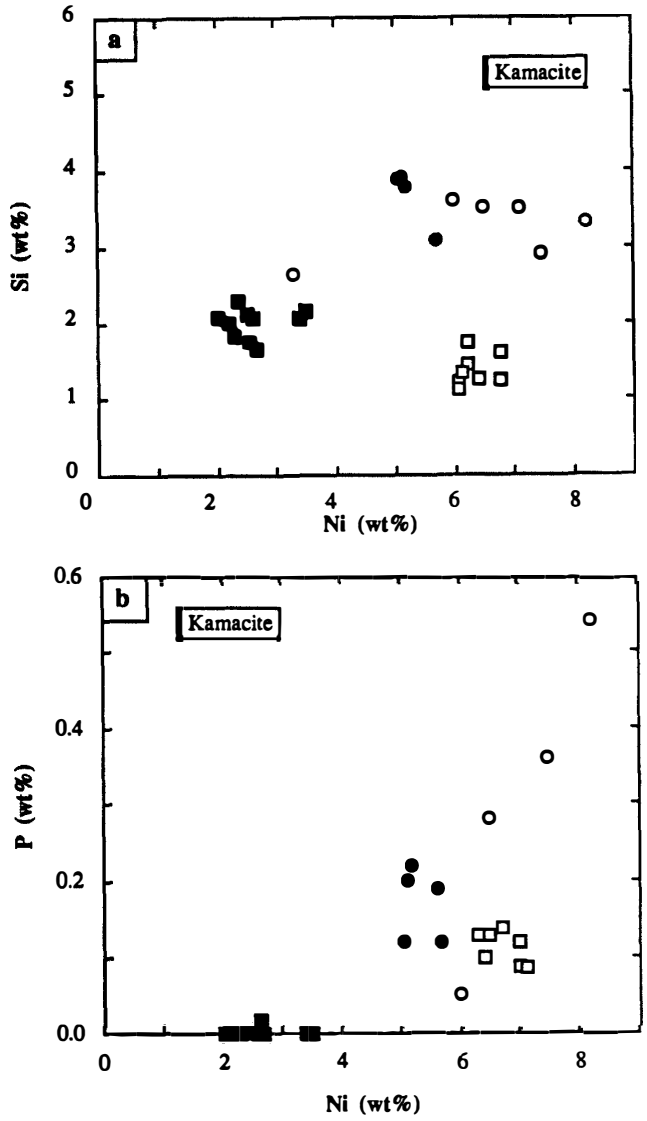

Fig. 4. The Ni-Si-P relationships of kamacite in Y-75261 in comparison with those in EH's, EL's, and Y-691 (EH3). Data source: KEIL (1968) and IKEDA (1989). Closed circle: Y-75261, open circle: EH chondrites, open square: EL chondrites, closed square: Y-691.

about 10 to 20 μm. It is rich in Cr (1.1–4.2 wt%) and Ti (0.2–0.8 wt%) (Table 5), which are higher than troilites in any other enstatite chondrites. The Cr and Ti contents are linearly related and are compared to those in EH and FL chondrites (Fig. 5). Figure 5a shows that the troilite in Y75261 has the similar Cr-Ti relationships to EH chondrites which is different from that for EL chondrites. The heterogeneity in Cr and Ti contents is among grains. No daubreelite lamellae have been found in Y-75261 on SEM images, but the very thin daubreelite lamellae may be responsible for the heterogeneity of Cr and Ti concentrations.

Troilite in the matrix is a fine (smaller than a few μm) bleb which is distributed in the clear glass and enstatite in the porphyritic portion (Fig. 2a). They are too small to be analyzed with a microprobe, and consequently it is not known whether the

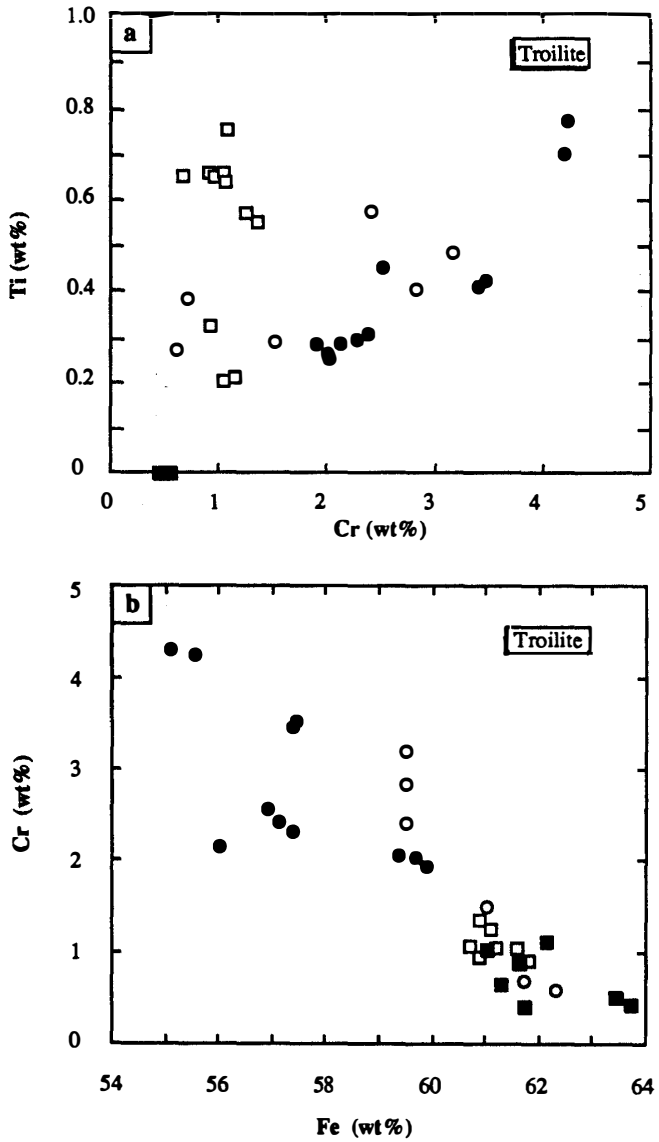

Fig. 5. The Cr-Ti-Fe relationships of troilite in Y-75261 in comparison with EH's, EL's, and Y-691. Data source: KEIL (1968) and EL GORESY et al. (1988). Closed circle: Y-75261, open circle: EH chondrites, open square: EL chondrites, closed square: Y-691.

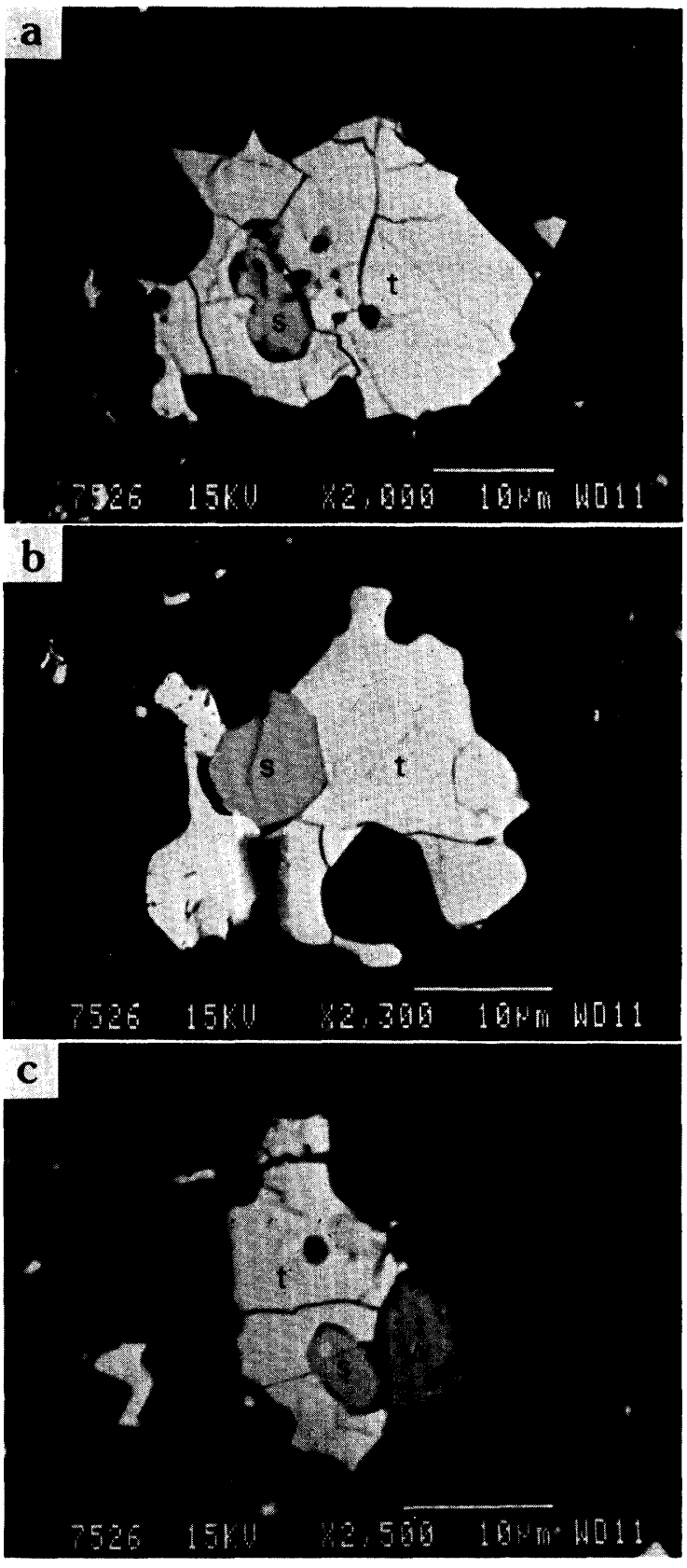

Fig. 6. BEI photographs showing occurrence of the monosulfide (FeMnMgCrCa) S. The monosulfide (s) usually accompanies troilite (t). W is a weathering product rich in Fe.

troilite in the matrix is chemically the same as that in the clast. The difference in grain size and shape, however, suggests that the troilites in clast and matrix are different in origin. Troilite in the matrix should have crystallized from a melt contrary to that in the matrix which appears to be fragmental.

The glassy groundmass contains a considerable amount of sulfur (Table 2). The absence of Fe in the melt, however, suggests that the sulfur was not derived from troilite but may be from oldhamite or niningerite. Since there is no correlation between the Ca and S contents in the glass, oldhamite is not the only precursor for sulfur.

The monosulfide is smaller than 10 μm mostly coexisting with troilite, which has a euhedral rectangular to ovoid shape enclosed in troilite (Fig. 6) and which is not exsolution lamellae from troilite. It has a stoichiometric composition, (Fe, Mn, Mg, Ca, Cr) S without Ti, though the Ca and Cr being accessory components. The chemical composition varies from grain to grain: 28–32 wt% Fe, 12–22 Mn, 6–11 Mg, 2–3 Ca, and 1–2 Cr (Table 5). It is not known whether the sulfide is heterogeneous within a grain or among grains because of the small size. The composition

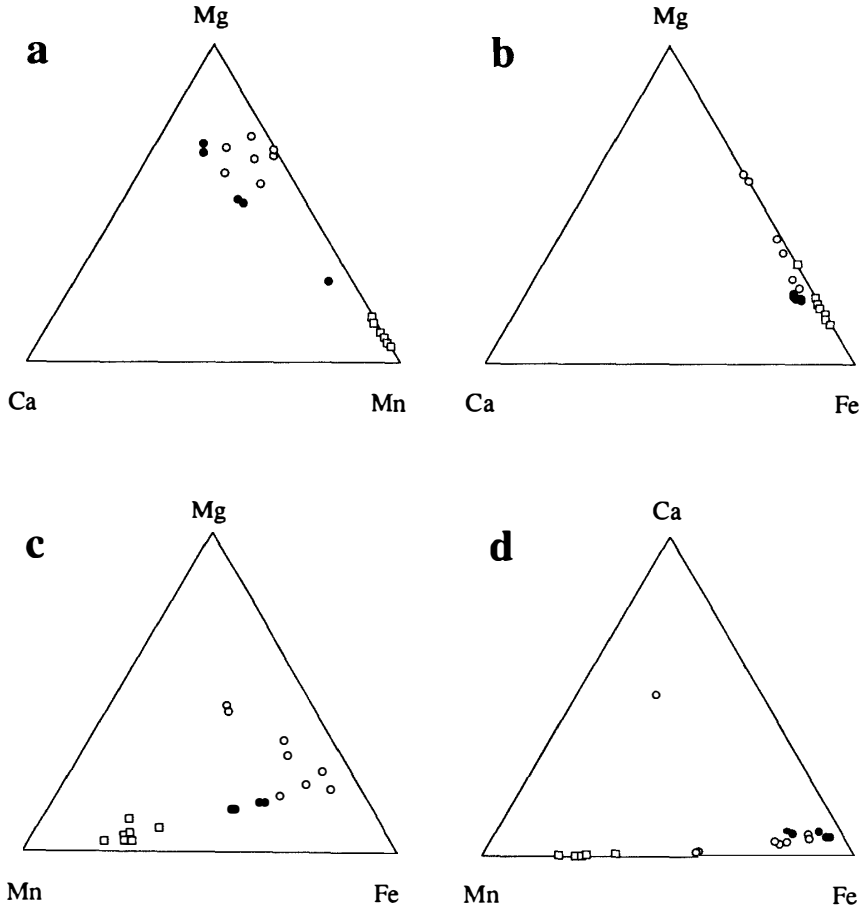

Fig. 7. Chemical composition of the monosulfide (FeMnMgCrCa) S plotted on the surfaces of the Fe-Mn-Mg-Ca tetrahedron projected from the apexes in comparison with niningerite in EL chondrites (data from KEIL, 1968). Closed circle: Y-75261, open circle: niningerites in EH chondrites, open square: alabandites in EL chondrites.

is intermediate between niningerites in EH chondrites and alabandites in EL chondrites. Figure 7 shows the composition of the monosulfide with niningerites in EH chondrites and alabandites in EL chondrites where Cr was excluded. They are plotted in the Fe-Mn-Mg-Ca tetrahedron, and projected on the four surfaces from the four apexes. The figure illustrates the anomalous composition of the sulfide. "Exotic niningerite" in Qingzhen enstatite chondrite (EHLERS and EL GORESY, 1988) is similar to the monosulfide in Y-75261 in that they have intermediate compositions between niningerite and alabandite, but differs in that the former is richer in Mg and poorer in Fe, Ca, and Cr than the latter. "Ferromagnesian alabandite" in the Norton County aubrite (OKADA *et al.*, 1988) also has a composition intermediate between niningerite and alabandite, but it is poorer in Fe, Mg, Ca, and richer in Mn.

There are two possibilities for the origin of the monosulfide. One is quenching from molten liquid, and the other is condensation at fairly high temperature. Since a sulfide with such a composition is supposed to be decomposed into several sulfides (troilite, niningerite, alabandite, oldhamite, and daubreelite) at temperatures below several hundreds °C (SKINNER and LUCE, 1971) and it decomposed fairly quickly, the sulfide should have been melted above the eutectic temperature and cooled rapidly. Coexistence of troilite and the monosulfide shows that the sulfide was quenched at temperatures a little below 1000°C (SKINNER and LUCE, 1971). This, however, appears to be implausible, because enstatite, the major constituent of the clast, is supposed to be formed by compaction but not crystallization from liquid. Hence, another possibility that the sulfide is a condensate may be plausible. Origin of the sulfide from condensate is consistent with texture of the clast. If this is the case, the clast should not have melted in spite of intensive melting of the matrix of the meteorite. Conditions for condensation of the sulfide (composition, temperature, and pressure of the gas) are not known.

5. Chemical Composition

Major elemental abundances of Y-75261 obtained with the broad beam technique of a microprobe are shown in Table 6 and Fig. 8 along with EH and EL chondrites by KALLEMEYN and WASSON (1986). Y-75261 exhibits large fractionation with respect to both lithophile and siderophile elements. The compositions of Y-75261 and those of the clast alone show similar patterns. Aluminum and Ca fractionation may be partly due to the analysis with the broad beam technique, but the degree of fractionation is much larger than the analytical error. Accordingly, the fractionation should be a primary feature of the meteorite. Although the reason for the Al-Ca fractionation is not known, it is consistent with the enrichment in Al and depletion in Ca in the interstitial material of the clast and the glass in the matrix. Depletion of siderophile elements (Fe and Ni) is conspicuous for Y-75261, which is also consistent with the apparent depletion of metallic iron over the thin section studied. Chromium is shown to be severely depleted in both the clast and bulk of Y-75261.

The elemental distributions of Si, Al, Mg, Fe, Ca, Na, and S in most part of the thin section studied are shown in Fig. 9. The relative distribution patterns of Si, Al, Ca, Na, and S are almost the same, which is opposite to those of Fe and Mg. Silica,

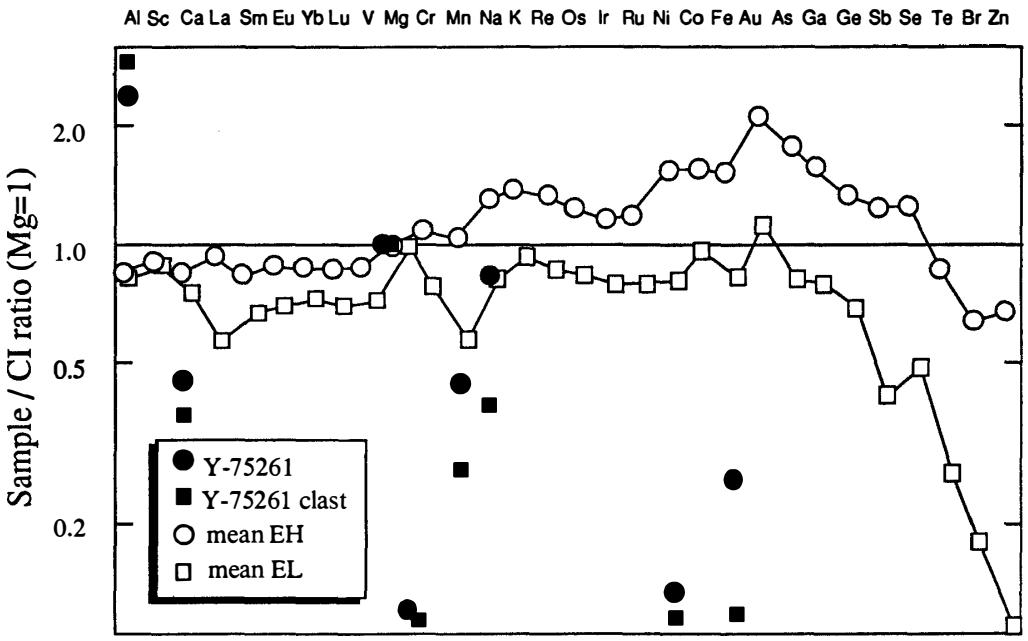

Fig. 8. Bulk chemical composition of Y-75261 and its clast alone in comparison with mean EH and EL chondrites. Analyses with the broad beam technique of a microprobe. Data for EH and EL chondrites are from KALLEMEYN and WASSON (1986).

Table 6. Chemical composition of the bulk, clast, and matrix portions of Y-75261 obtained by the broad beam technique of a microprobe.

	SiO_2	TiO_2	Al_2O_3	FeO	MnO	MgO	CaO	Na_2O	Cr_2O_3	NiO	S	Total
Bulk 1	46.80	0.00	8.60	5.00	0.26	28.80	1.30	0.99	0.00	0.54	1.10	94
Bulk 2	47.10	0.00	7.70	4.10	0.21	29.90	1.00	0.86	0.00	0.00	1.10	93
Clast	49.30	0.00	8.10	3.40	0.12	32.40	0.86	0.49	0.00	0.33	0.90	96
Matrix	51.30	0.00	8.70	4.40	0.16	27.80	2.10	1.60	0.00	0.46	1.60	98

"Bulk 1" and "bulk 2" are different analyses for the whole sample. Results are normalized to 100% and the original total is shown in the last column.

Al, Ca, Na, and S are enriched in the matrix and the clast is enriched in Mg. Silica enrichment of the matrix is due to its origin as a residual liquid after crystallization of forsterite. The Mg-rich and Ca-, Na- and S-poor nodular portions embedded in the matrix are the aggergates of phenocrysts. The boundary between the clast and the matrix is clearly shown in most figures, especially for Na. The sharp boundary between the clast and the matrix does not completely correspond to that between glass-present and glass-absent portions. If the chemical fractionation between the matrix and the clast was caused by mobilization of elements during partial melting of the meteorite by a shock, the distribution of glass and chemical heterogeneity should correspond to each other. The fact that the distribution of glass does not completely correspond to that of elements enriched in glass, however, shows that the melting that formed glass is not responsible for elemental fractionation in the meteorite. In other words, the clast-matrix relationship was original; that is, the brecciated texture had been established before the shock which melted the matrix heterogeneously.

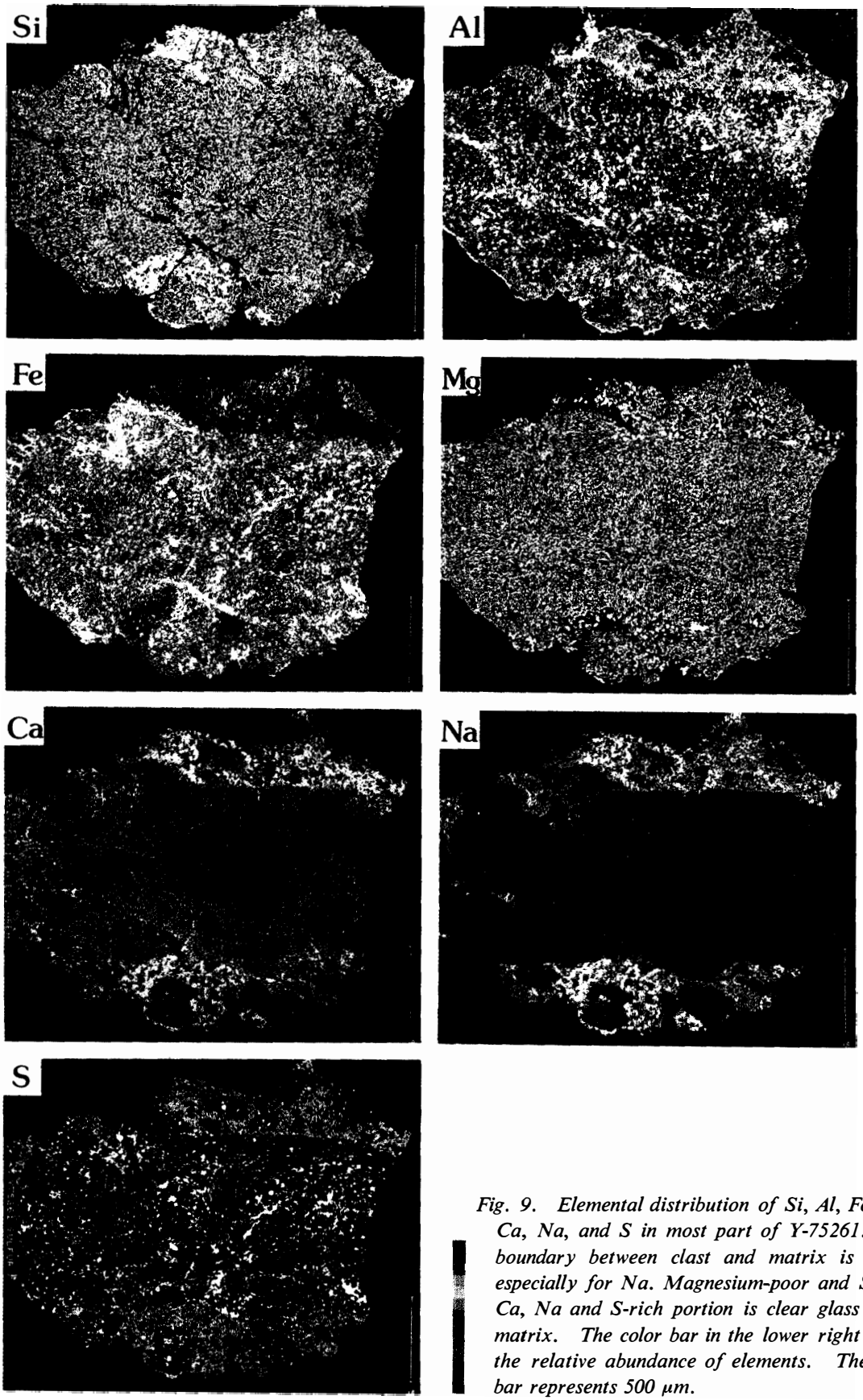

Fig. 9. Elemental distribution of Si, Al, Fe, Mg, Ca, Na, and S in most part of Y-75261. The boundary between clast and matrix is sharp, especially for Na. Magnesium-poor and Si, Al, Ca, Na and S-rich portion is clear glass of the matrix. The color bar in the lower right shows the relative abundance of elements. The scale bar represents 500 μm.

6. Discussion

It is evident from the texture and heterogeneous distrbution of glass that Y-75261 had been once shocked to partially melt. Highly magnesian pyroxene, essential absence of olivine, and the presence of the Mn-Fe-Mg-Ca-Cr monosulfide shows that the meteorite is genetically related to enstatite chondrites. Chemical compositions of pyroxene, kamacite, and troilite (Figs. 3–5) suggest the closer relationship to EH chondrites than to EL chondrites. Although Y-75261 may be related to EH chondrites, the bulk composition of Y-75261 is not chondritic. A possible expanation for the siderophile depletion is small size of the sample studied, which may not be representative of the meteorite.

Strong depletion of metallic iron is often the case in enstatite chondrite breccias. "Impact melt-rock clasts" in Hvittis (RUBIN, 1983a) seem to be similar to the breccia in Y-75261 in that both are fine-grained and depleted in metallic iron and sulfide. But they differ in that the clasts in Hvittis have daubreelite, alabandite, and oldhamite though the breccia in Y-75261 has monosulfide which can be stable at higher temperatures. In addition to the sulfide, the matrices of Y-75261 and Hvittis are quite different: the matrix of Hvittis has plagioclase which is absent in Y-75261. Presence of three sulfides and plagioclase in Hvittis suggests that Hvittis cooled more slowly than Y-75261 from the melting temperature to several hundreds °C. Atlanta (RUBIN, 1983b), Brithfield (RUBIN, 1984), Adhi Kot (RUBIN, 1983c), and Abee (RUBIN and KEIL, 1983) are breccias. These breccias are similar to that in Y-75261 and the clast in Hvittis in that all of them are depleted in metallic iron, but differ in that they have abundant troilite although troilite is almost absent in the clasts in Y-75261 and Hvittis.

It is a problem whether Y-75261 had primarily been a breccia which had been shocked to partly melt later on or the brecciated texture was formed by a shock. As mentioned before, Fig. 9 suggests that the brecciated texture of Y-75261 could have been established before partial melting of the matrix. If it is the case, the chemical fractionation between the clast and the matrix should have originated when the texture of the breccia was formed. Melting of some portions of the matrix did not largely change the elemental distribution.

The texture of the clast that the euhedral to subhedral enstatite grains with nearly the same size and smaller amounts of interstitial material are closely packed is suggestive of generation of the clast by compaction in a solid state. The presence of monoclinic pyroxene does not necessarily imply that it crystallized from a melt. Pyroxene experimentally condensed from a gas with non-chondritic composition is monoclinic (NAGAHARA *et al.*, 1988), and consequently the monoclinic pyroxene in the clast could be a condensate. The monosulfide should also be a condensate, as mentioned before.

The interstitial material of the clast is rich in Al_2O_3. Aluminum-rich but Ca-poor material is not common in meteorites except for Ca-Al-rich inclusions and Ca-Al-rich chondrules. Groundmass of common chondrules is rich in Si but is not so much enriched in Al. Enormously Al-rich material could not be residual liquid after crystallization of enstatite from chondritic precursor. This is also supported by the texture of the clast that the pyroxene is not porphyritic against the Al-rich material.

The texture of the clast is rather suggestive of compaction, which in turn represents that the Al-rich material should have been present as isolated fragments. If the Al_2O_3-rich material was not a residual liquid, the alternative possibility is a condensate. Aluminum-rich material could be condensed from the gases of the solar or non-solar compositions with various total pressure and C/O ratios at high temperatures (LATTIMER *et al.*, 1978). Both enstatite and interstitial material of the clast may thus have been condensates at high to medium temperatures. In this case, essential absence of Ca in the interstitial material should be explained by high temperature fractionation. Aluminum and Ca can be fractionated effectively under reducing conditions than oxidizing conditions: condensation temperature difference between corundum and melilite is larger or Ca condenses as CaS in reducing conditions. Calcium could have been fractionated from the meteorite with the loss of sulfur, though of which mechanism is hardly known.

In conclusion, Y-75261 is a regolith breccia of EH chondrite parent body having a clast which was made up of compacted condensates. The meteorite was shocked to partly melt at above 1000°C and under a fairly oxidizing condition to form porphyritic texture in the matrix. It cooled quickly, almost quenched, which may correspond to excavation of the meteorite from the parent body.

Acknowledgments

The comments by two anonymous reviewers are greatly appreciated. Efforts by the consortium leader, I. KUSHIRO, K. YANAI, and H. KOJIMA are thanked. This paper is part of a consortium study on unique Antarctic meteorites.

References

EHLERS, K. and EL GORESY, A. (1988): Normal and reverse zoning in niningerite: A novel key parameter to the thermal histories of EH-chondrites. Geochim. Cosmochim. Acta, **52**, 877–887.

EL GORESY, A., YABUKI, H., WOOLUM, D. and PERNICKA, E. (1988): Qingzhen and Y-691: A tentative alphabet for the EH chondrites. Proc. NIPR Symp. Antarct. Meteorites, **1**, 65–101.

IKEDA, Y. (1989): Petrochemical study of the Yamato-691 enstatite chondrite (E3) IV: Descriptions and mineral chemistry of opaque-mineral nodules. Proc. NIPR Symp. Antarct. Meteorites, **2**, 109–146.

KALLEMEYN, G. W. and WASSON, J. T. (1986): Compositions of enstatite (EH3, EH4, 5 and EL6) chondrites: Implications regarding their formation. Geochim. Cosmochim. Acta, **50**, 2153–2164.

KEIL, K. (1968): Mineralogical and chemical relationships among enstatite chondrites. J. Geophys. Res., **73**, 6945–6976.

LATTIMER, J. M., SCHRAMM, D. N. and GROSSMAN, K. (1978): Condensation in supernova ejecta and isotopic anomalies in meteorites. Astrophys. J., **219**, 230–249.

MAYEDA, T. K. and CLAYTON, R. N. (1989): Oxygen isotopic composition of unique Antarctic meteorites. Paper Presented to the 14th Symposium on Antarctic Meteorites, June 6–8, 1989. Tokyo, Natl Inst. Polar Res., 172.

NAGAHARA, H., KUSHIRO, I., MYSEN, B. O. and MORI, H. (1988): Experimental vaporization and condensation of olivine solid solution. Nature, **331**, 516–518.

NAGAHARA, H., FUKUOKA, T., KANEOKA, I., KIMURA, M., KOJIMA, H., KUSHIRO, I., TAKEDA, H.,

TSUCHIYAMA, A. and YANAI, K. (1990): Petrology of unique meteorites, Y-74063, Y-74357, Y-75261, Y-75274, Y-75300, A-77081, A-78230, and Y-8002. Paper Presented to the 15th Symposium on Antarctic Meteorites, May 30–June 1, 1990. Tokyo, Natl Inst. Polar Res., 92–94.

OKADA, A., KEIL, K., TAYLOR, G. J. and NEWSOM, H. (1988): Igneous history of the aubrite parent asteroid: Evidence from the Norton County enstatite achondrite. Meteoritics, **23**, 59–74.

RUBIN, A. E. (1983a): Impact melt-rock clasts in the Hvittis enstatite chondrites breccia: Implication for a genetic relationship between EL chondrites and aubrites. Proc. Lunar Planet. Sci. Conf., 14th, Pt. 1, B293–B300 (J. Geophys. Res., **88** Suppl.).

RUBIN, A. E. (1983b): The Atlanta enstatite chondrite breccia. Meteoritics, **18**, 113–121.

RUBIN, A. E. (1983c): The Adhi Kot breccia and implications for the origin of chondrules and silica-rich clasts in enstatite chondrites. Earth Planet. Sci. Lett., **64**, 201–212.

RUBIN, A. E., (1984): The Blithfield meteorite and the origin of sulfide-rich, metal-poor clasts and inclusions in brecciated enstatite chondrites. Earth Planet. Sci. Lett., **67**, 273–283.

RUBIN, A. E. and KEIL, K. (1983): Mineralogy and petrology of the Abee enstatite chondrite breccia and its dark inclusions. Earth Planet. Sci. Lett., **62**, 118–131.

SKINNER, B. J. and LUCE, F. D. (1971): Solid solution of the type (Ca, Mg, Mn, Fe) S and their use as geothermometers for the enstatite chondrites. Am. Mineral., **56**, 1269–1296.

YANAI, K. and KOJIMA, H. (1985): Meteorites News, Jpn. Coll. Antarct. Meteorites, **4**(1), 6.

(Received August 9, 1990; Revised manuscript received October 16, 1990)